

## What can we learn from the Fourier analysis of Blazar light curves?

**Justin D. Finke (NRL)**

**Peter A. Becker (GMU)**

**Tiffany Lewis (GMU)**

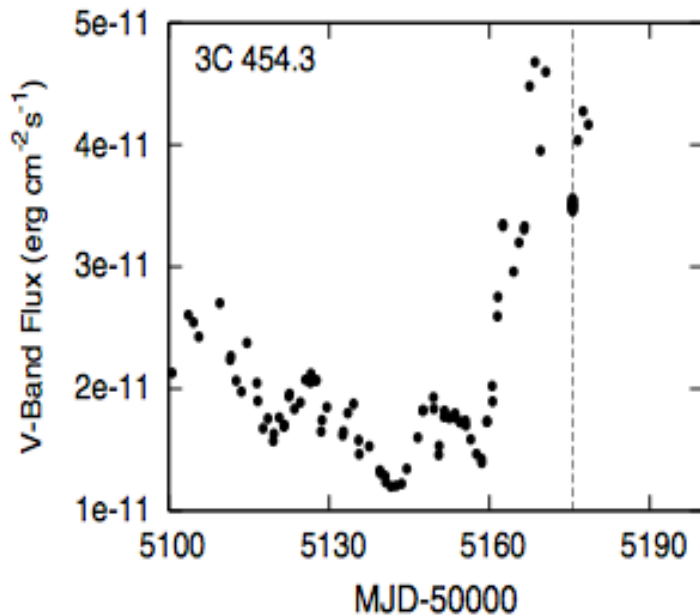
**24 April 2015**

Finke & Becker (2014), ApJ,  
791, 21

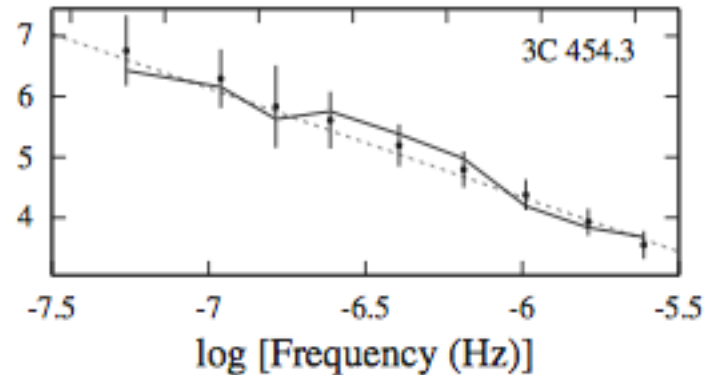
Finke & Becker (2015),  
submitted

Lewis, Becker, & Finke (2015) in  
preparation

# Characterizing Variability



Fourier  
transform



Chatterjee et al. (2012), ApJ, 749, 191

$$\text{PSD: } S(f) = |\tilde{x}(f)|^2 = \tilde{x}(f)\tilde{x}^*(f)$$

Power spectral densities (PSDs) of blazars are consistent with red noise, i.e., power laws.

Variability appears to be **stochastic**.

Can we make any theoretical predictions for blazar PSDs?

# Continuity Equation



Blazar variability often described by electron continuity equation

$$\frac{\partial N_e}{\partial t} + \frac{\partial}{\partial \gamma} [\dot{\gamma}(\gamma, t) N_e(\gamma; t)] + \frac{N_e(\gamma; t)}{t_{\text{esc}}(\gamma, t)} = Q(\gamma, t)$$

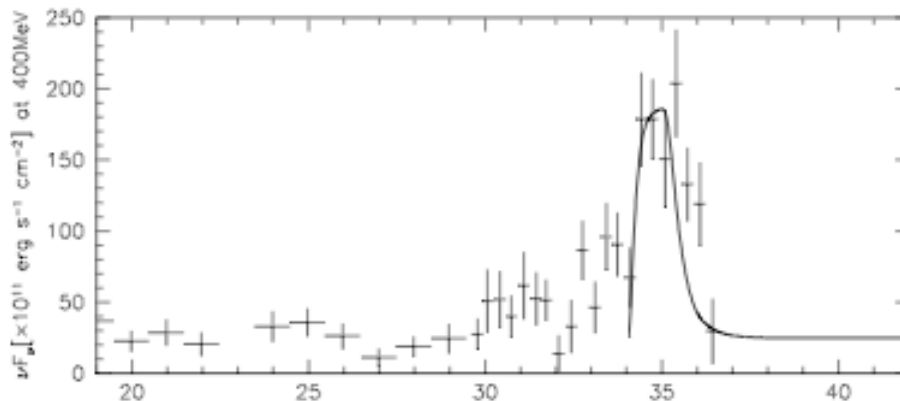
Cooling from synchrotron and Compton scattering

Electron escape

Electron distribution

Electron injection

Standard modeling of individual flares: Choose  $Q(\gamma, t)$  and solve for  $N_e(\gamma; t)$ , the electron distribution, useful for simulating individual flares (e.g., Mastichiadis & Kirk 1995; Chiaberge & Ghisellini 1999; Li & Kusunose 2000; Boettcher & Chiang 2002).



3C 279; Moderski et al. (2003),  
A&A, 406, 855

What about the Fourier  
transform and PSDs?

# Fourier Transform



We'll assume all variability comes only from variations in electron injection.

Take Fourier transform of continuity equation:

$$-2\pi i f \tilde{N}_e(\gamma, f) + \frac{\partial}{\partial \gamma} [\dot{\gamma}(\gamma) \tilde{N}_e(\gamma, f)] + \frac{\tilde{N}_e(\gamma, f)}{t_{\text{esc}}(\gamma)} = \tilde{Q}(\gamma, f)$$

Fourier-  
transformed  
electron injection  
term

Fourier-  
transformed  
electron  
distribution

Tilde indicates Fourier transform. Time-derivative has been eliminated, and this ODE has a relatively simple solution.

PSDs of blazars are power-laws, and power-laws in electron energy are standard. So we will guess that particle injection is a power-law in frequency and energy:

$$\tilde{Q}(\gamma, f) = Q_0 (f/f_0)^{-a/2} \gamma^{-q} H(\gamma; \gamma_1, \gamma_2) H(f; f_1, f_2)$$

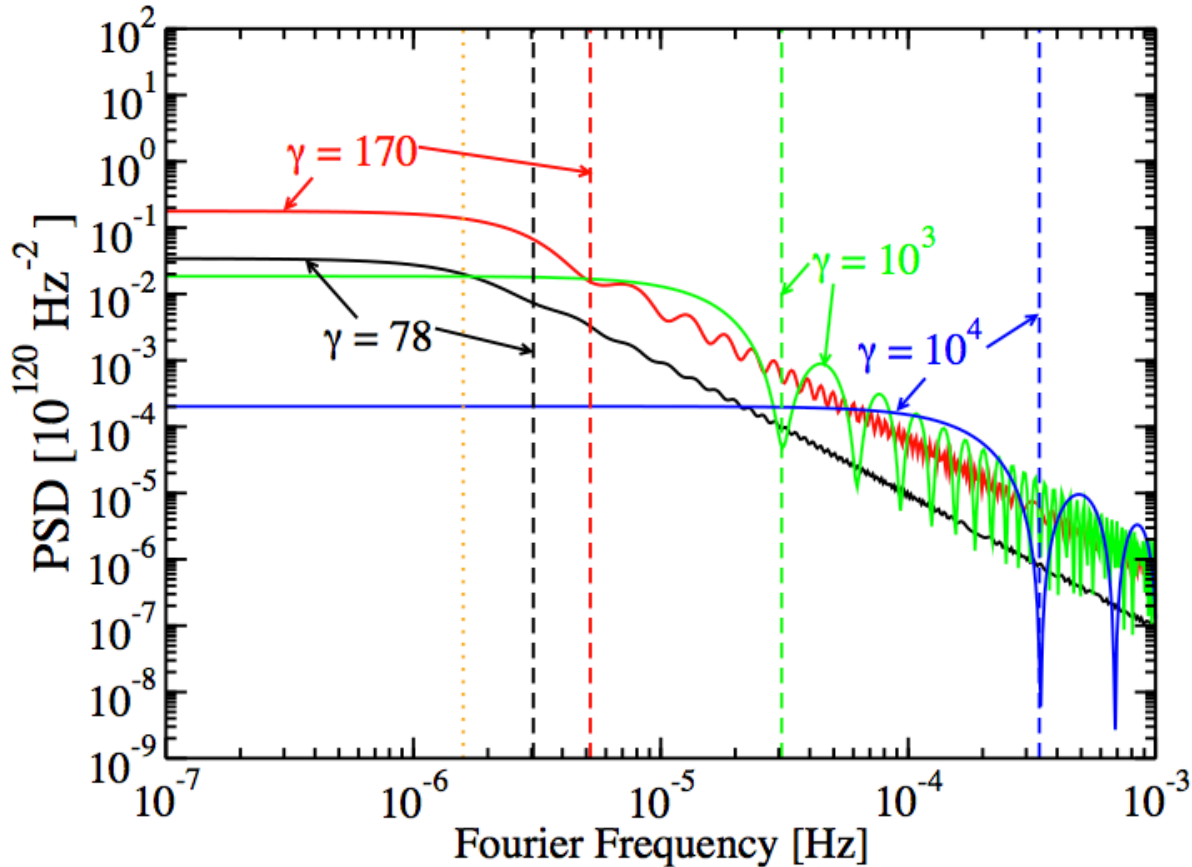
Solve equation for  $\tilde{N}_e(\gamma, f)$ .

# PSD for electron distribution



For synchro-Thomson losses:

For low  $\gamma$ , break at  $f=1/(2\pi t_{\text{esc}})$



For large  $\gamma$ , break at  $f=1/(t_{\text{cool}})$ . Also sinusoidal features at integer values of  $f=1/(t_{\text{cool}})$ .

Variability on timescales shorter than cooling timescale is not preferred.

In all cases, break is from  $f^{-a}$  to  $f^{-(a+2)}$

Fig. 1.— The PSD from Equation (17) for  $q = 2$ ,  $a = 0$ ,  $t_{\text{esc}} = 10^5$  s,  $\nu = 3.1 \times 10^{-8}$  s $^{-1}$ ,  $\langle L_{\text{inj}} \rangle = 10^{42}$  erg s $^{-1}$ ,  $\Delta t = 1$  year,  $\gamma_1 = 10^2$ ,  $\gamma_2 = 10^5$ . Dashed lines indicate  $f = t_{\text{cool}}^{-1}$  for each curve, and the dotted line indicates  $f = (2\pi t_{\text{esc}})^{-1}$ .

## Emission and light travel time



We assume blob is entirely homogeneous. Variations take place throughout blob simultaneously.

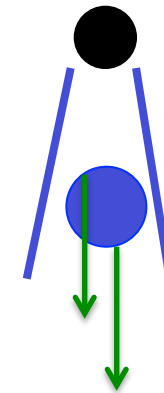
However, even in this case, photons from closer part of the “blob” will reach earth before those from the farther part. For synchrotron or external Compton ( $\delta$ -function approximation):

$$F_{\epsilon}(t) = \frac{K(1+z)}{t_{lc}\delta_D} \int_0^{2R'/c} dt' N_e \left( \gamma'; \frac{t\delta_D}{1+z} - t' \right)$$

where  $t_{lc} = \frac{2R'(1+z)}{c\delta_D}$  e.g., Chiaberge & Ghisellini (1999)  
Zacharias & Schlickeiser (2013)

So what will the PSD of the flux look like?

$$S(\epsilon, f) = |\bar{F}_{\epsilon}(f)|^2 = \frac{K^2(1+z)^2}{(\pi f t_{lc} \delta_D)^2} \left| \tilde{N}_e \left( \gamma', \frac{(1+z)f}{\delta_D} \right) \right|^2 \sin^2(\pi f t_{lc})$$

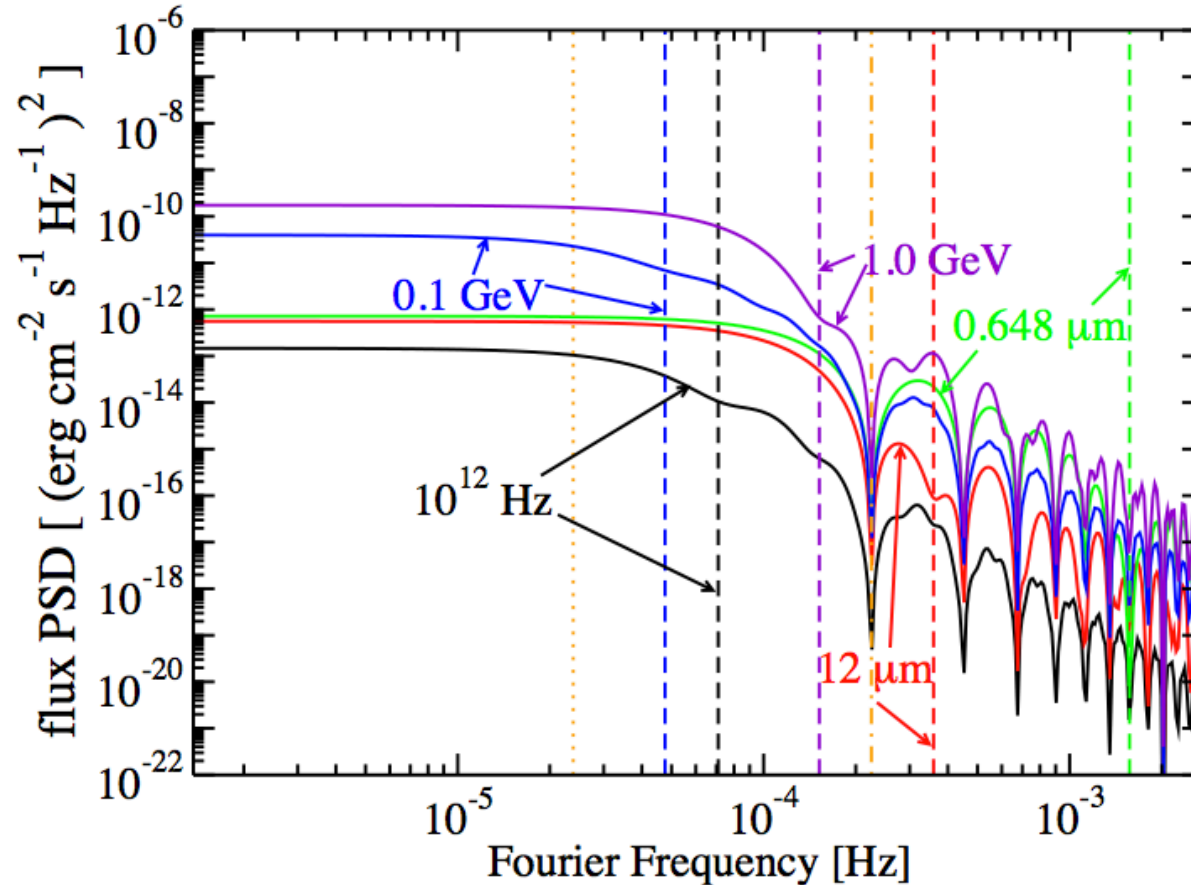


blazar



Earth

## Theoretical Flux PSDs



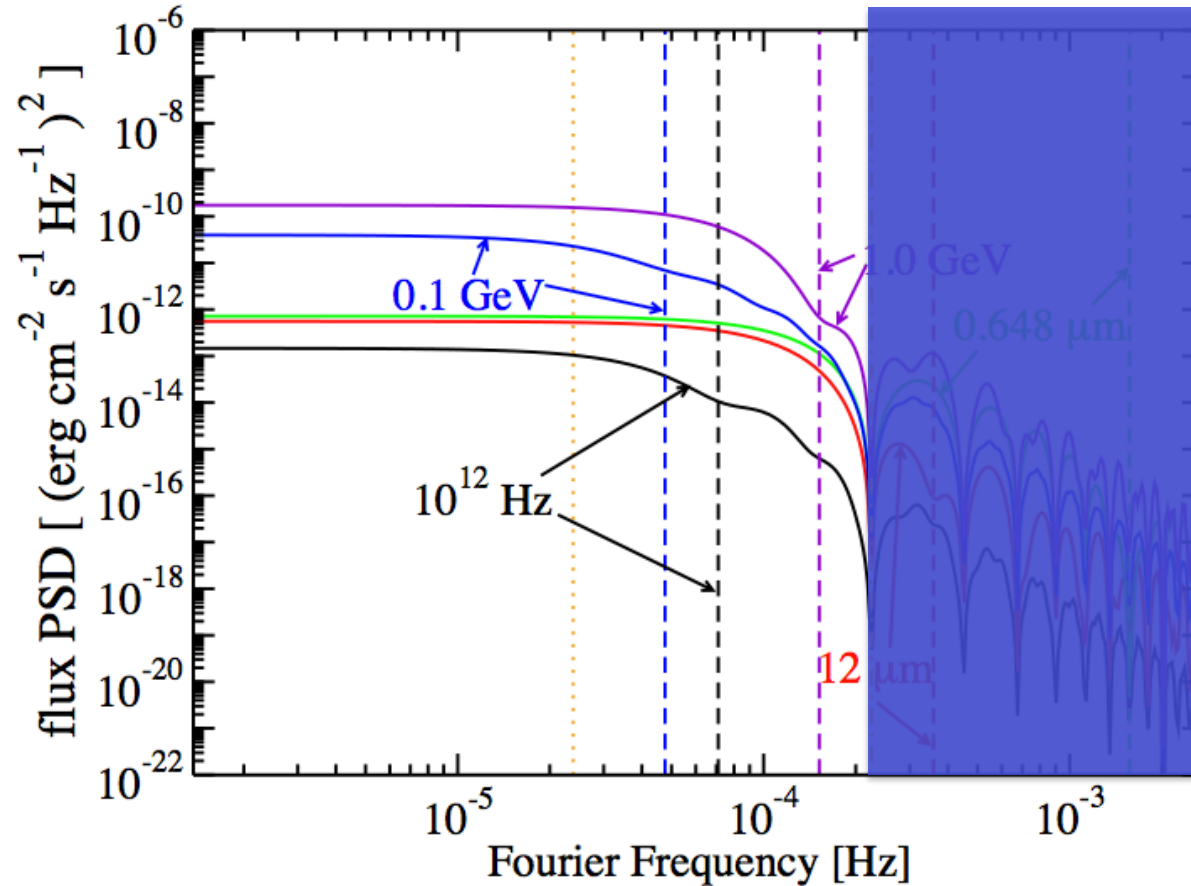
Synchrotron and EC PSDs.

Same features from electron PSD are seen. Namely, for low  $\gamma$ , break at  $f=1/(2\pi t_{\text{esc}})$ , sinusoidal features at  $f=1/t_{\text{cool}}$ .

Additionally, features at integer values of  $f=1/t_{\text{lc}}$  in all PSDs.

Fig. 4.— The flux PSD computed from Equations (45) and (17) using the same parameters as in Figure 1. Additional parameters are  $\delta_D = \Gamma = 30$ ,  $B = 1$  G,  $u_0 = 10^{-3}$  erg cm $^{-3}$ ,  $\epsilon_0 = 2 \times 10^{-5}$ ,  $R' = 10^{15}$  cm, and  $z = 1$ . At this redshift with a cosmology  $(h, \Omega_m, \Omega_\Lambda) = (0.7, 0.3, 0.7)$ ,  $d_L = 2 \times 10^{28}$  cm. The observed photon frequency, wavelength, or energy is shown, along with  $t_{\text{cool}}^{-1}$  for each curve (dashed lines),  $(2\pi t_{\text{esc}})^{-1}$  (dotted line), and  $t_{\text{lc}}^{-1}$  (dashed-dotted line), all computed in the observer's frame.

# Theoretical Flux PSDs



Synchrotron and EC PSDs.

Unphysical region?

Fig. 4.— The flux PSD computed from Equations (45) and (17) using the same parameters as in Figure 1. Additional parameters are  $\delta_D = \Gamma = 30$ ,  $B = 1$  G,  $u_0 = 10^{-3}$  erg cm $^{-3}$ ,  $\epsilon_0 = 2 \times 10^{-5}$ ,  $R' = 10^{15}$  cm, and  $z = 1$ . At this redshift with a cosmology  $(h, \Omega_m, \Omega_\Lambda) = (0.7, 0.3, 0.7)$ ,  $d_L = 2 \times 10^{28}$  cm. The observed photon frequency, wavelength, or energy is shown, along with  $t_{\text{cool}}^{-1}$  for each curve (dashed lines),  $(2\pi t_{\text{esc}})^{-1}$  (dotted line), and  $t_{\text{lc}}^{-1}$  (dashed-dotted line), all computed in the observer's frame.

# Theoretical Flux PSDs

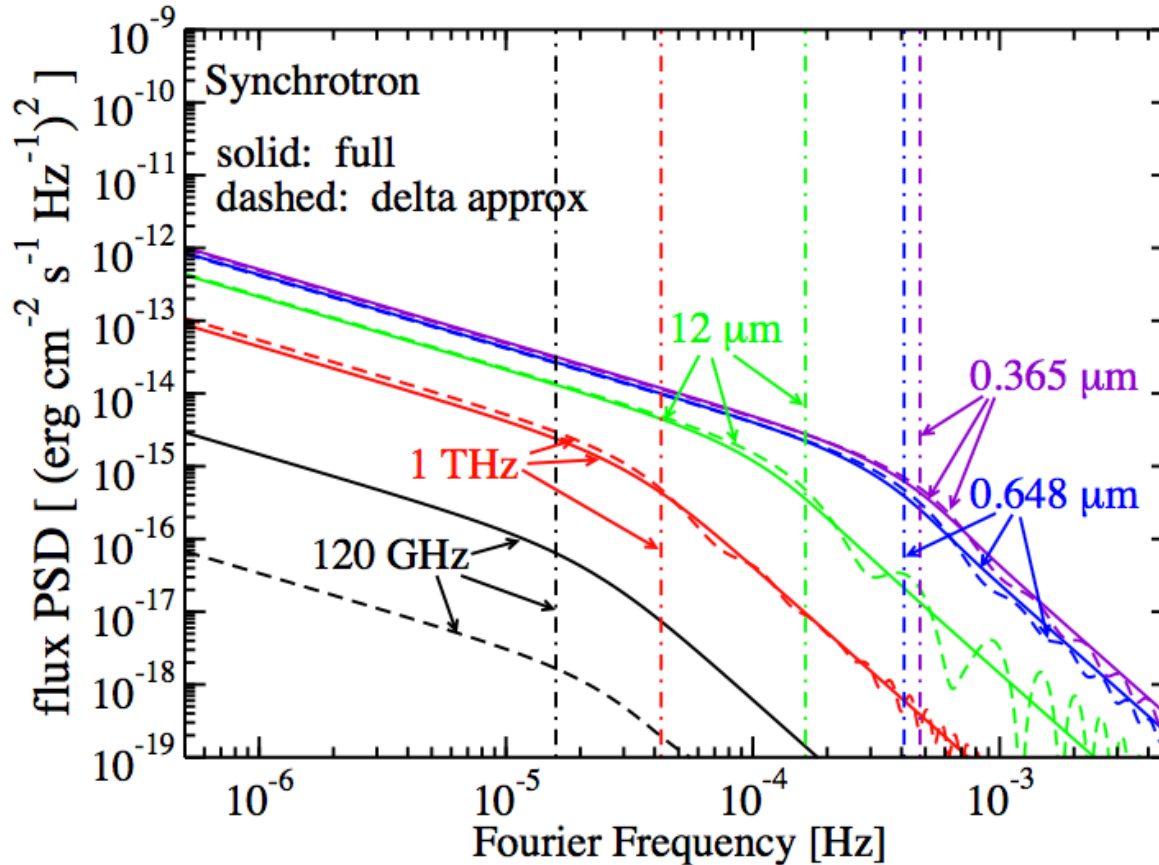


Fig. 1.— The synchrotron PSD for the  $\delta$ -function approximation (dashed curves) and full calculation (solid curves). Parameters are  $q = 2$ ,  $a = 1$ ,  $t_{\text{esc}} = 10^5$  s,  $\langle L_{\text{inj}} \rangle = 10^{42}$  erg s<sup>-1</sup>,  $\Delta t = 1$  year,  $\gamma_1 = 10^2$ ,  $\gamma_2 = 10^5$ ,  $R' = 10^{15}$  cm,  $B = 1$  G,  $\Gamma = \delta_D = 30$ ,  $u_0 = 10^{-3}$  erg cm<sup>-3</sup>,  $\epsilon_0 = 5 \times 10^{-7}$ , and  $z = 1$ . At this redshift with cosmology  $(h, \Omega_m, \Omega_\Lambda) = (0.7, 0.3, 0.7)$  the luminosity distance  $d_L = 2 \times 10^{28}$  cm. The observed photon frequency or wavelength is shown. Dashed-dotted lines indicate  $f = (1.5t_{\text{cool}})^{-1}$  for each curve.

Minima features are washed out when full calculation is used.

PSDs resemble broken power-laws. Break is from  $f^{-a}$  to  $f^{-(a+2)}$ .

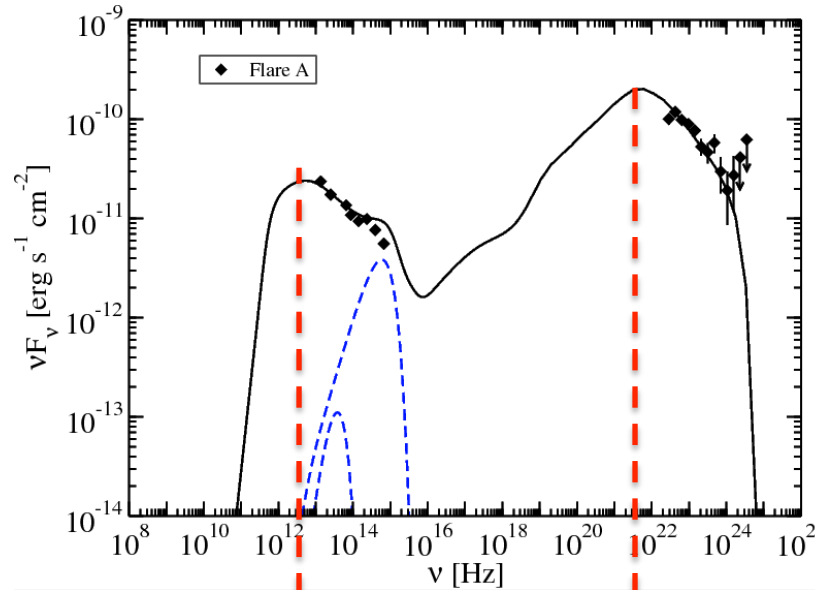
PSDs from electrons with energies  $\gamma < \gamma_1$  are not accurate with  $\delta$ -function approximation (120 GHz curve).

Similar results for EC.

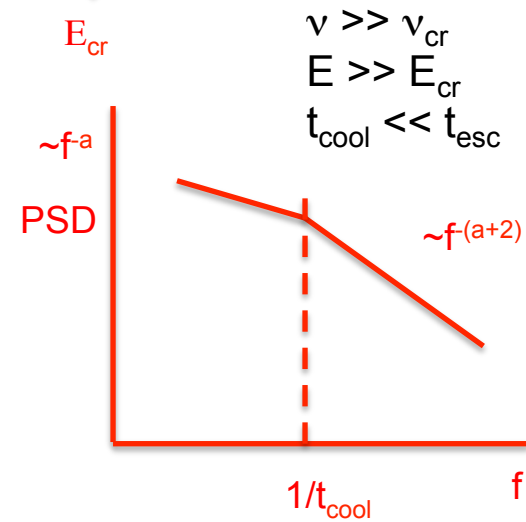
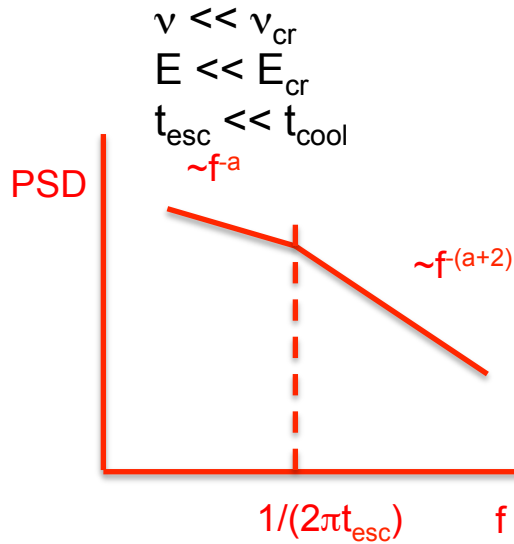
# PSD Observer's Summary



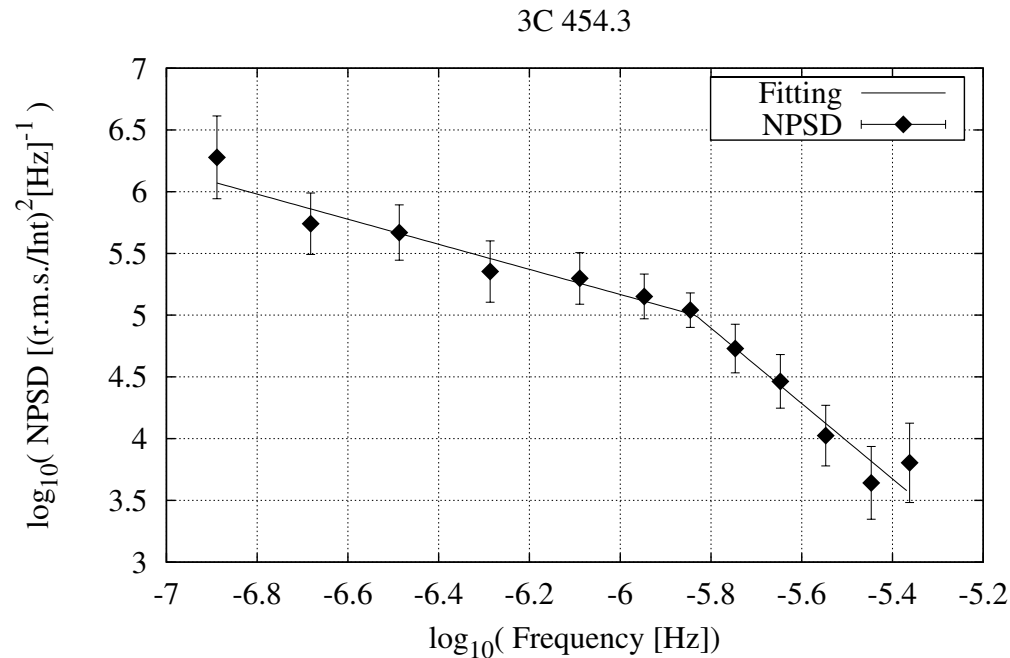
If SED peak is associated with  
where  $t_{\text{cool}} = t_{\text{esc}}$



PKS 2142-75; Dutka et al. (2013), ApJ, 779, 714



# The Observed $\gamma$ -ray PSD of 3C 454.3



A break is seen in the LAT PSD of 3C 454.3!

PSD goes from  $\sim f^{-1}$  to  $f^{-3}$ , as theory predicts!

Break frequency:  $1.5 \times 10^{-6}$  s, corresponding to 7.9 days

How can this be resolved with light curves of bright flares, where decays are seen on timescales of several hours?

Nakagawa & Mori (2013), ApJ, 773, 177

## The Observed PSD of 3C 454.3



If break is associated with cooling timescale:

$$\begin{aligned}
 u_0 &\approx \frac{3m_e c^2}{4c\sigma_T \Gamma^2 t'_{\text{cool}} \gamma'} = 9.6 \times 10^{-6} \left(\frac{\Gamma}{30}\right)^{-2} \left(\frac{E}{100 \text{ MeV}}\right)^{-1/2} && \text{(dust torus)} \\
 &\quad \times \left(\frac{\epsilon_0}{5 \times 10^{-7}}\right)^{1/2} \text{ erg cm}^{-3} \\
 &= 6.1 \times 10^{-5} \left(\frac{\Gamma}{30}\right)^{-2} \left(\frac{E}{100 \text{ MeV}}\right)^{-1/2} && \text{(broad line region)} \\
 &\quad \times \left(\frac{\epsilon_0}{2 \times 10^{-5}}\right)^{1/2} \text{ erg cm}^{-3}, \quad (73)
 \end{aligned}$$

If break is associated with escape timescale:

$$t'_{\text{esc}} = 20 \text{ days} \left(\frac{\delta_D}{30}\right).$$

$$R_b' < 10^{18} \text{ cm}$$

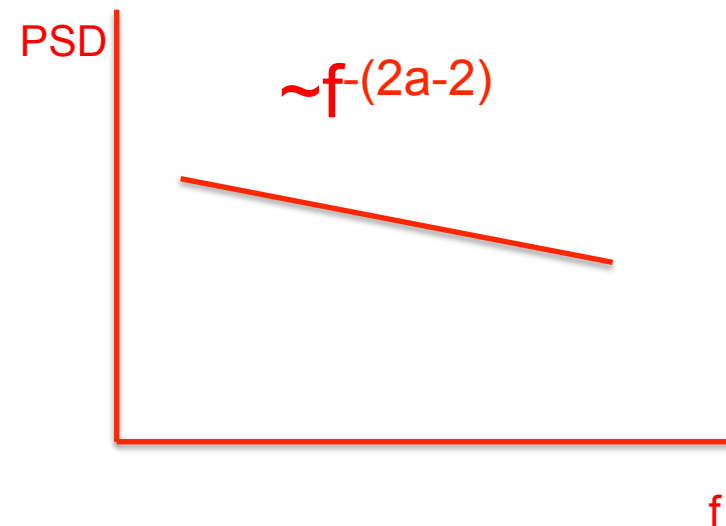
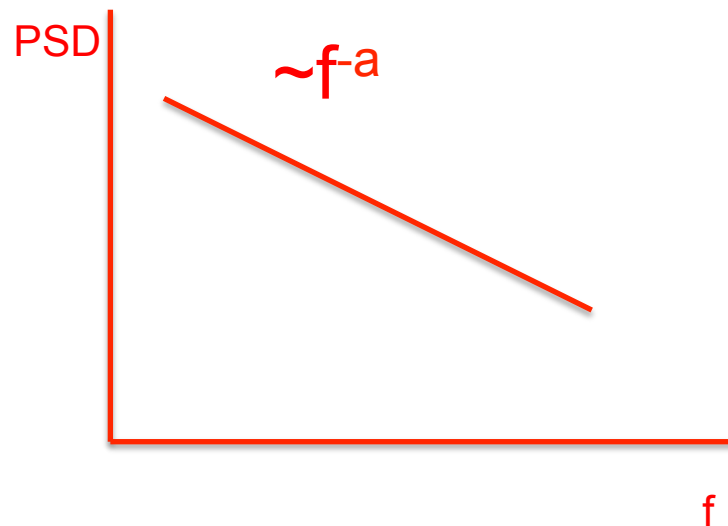


***That is for synchrotron and External Compton (EC). What about synchrotron self-Compton (SSC)?***

*That is for synchrotron and External Compton (EC). What about synchrotron self-Compton (SSC)?*

Synch/EC

SSC



Recall  $Q(\gamma, f) \sim f^a$

# Observed Gamma-ray PSDs



If  $a$  is roughly the same for all blazars, what would we expect to observe in the PSDs of blazars' gamma-ray (*Fermi*-LAT) light curves?

Observed PSD:  $S \sim f^b$

FSRQs  $\longrightarrow$  External Compton  $\longrightarrow$   $b = a$

BL Lacs  $\longrightarrow$  Synchrotron self-Compton  $\longrightarrow$   $b = 2a - 2$

So we predict that generally, **FSRQs** should have **steeper** PSDs than **BL Lacs** if  $a < 2$ .

*Is this observed?*

# Gamma-ray PSD indices



**Table 1**

*Fermi*-LAT PSD Power-law Indices ( $b$ ) from Nakagawa & Mori (2013) and the Values of  $a$  from Our Model Needed to Reproduce Them

Object	$b$	$a$
FSRQs		
4C +28.07	$0.93 \pm 0.23$	0.93
PKS 0426–380 <sup>a</sup>	$1.16 \pm 0.47$	1.16
PKS 0454–234	$0.78 \pm 0.27$	0.78
PKS 0537–441 <sup>a</sup>	$0.86 \pm 0.64$	0.86
PKS 1222+216	$0.65 \pm 0.21$	0.65
3C 273	$1.30 \pm 0.27$	1.30
3C 279	$1.23 \pm 0.35$	1.23
PKS 1510–089	$1.10 \pm 0.30$	1.10
3C 454.3	$1.00 \pm 0.24$	1.00
PKS 2326–502	$1.26 \pm 0.44$	1.26
Mean	1.01	1.01
S.D.	0.26	0.26
BL Lac Objects		
3C 66A	$0.60 \pm 0.44$	1.22
Mrk 421	$0.38 \pm 0.21$	1.19
PKS 2155–304	$0.58 \pm 0.33$	1.29
BL Lac	$0.41 \pm 0.47$	1.21
Mean	0.49	1.23
S.D.	0.11	0.07

**Note.** <sup>a</sup> PKS 0426–380 and PKS 0537–441 were previously classified as BL Lac objects.

Essentially all FSRQs have PSD index consistent with  $b=1$  (within errors)

Essentially all BL Lacs have PSD index consistent with  $b=0.5$ .

In general agreement with our model if FSRQs make  $\gamma$  rays from EC and BL Lacs make  $\gamma$  rays from SSC.

Categorized as BL Lacs or FSRQs based on Ghisellini et al. (2011) MNRAS, 414, 2674.  
Boundary at  $L_{\text{BLR}} / L_{\text{Edd}} = 5 \times 10^{-4}$

# Full Compton cross-section

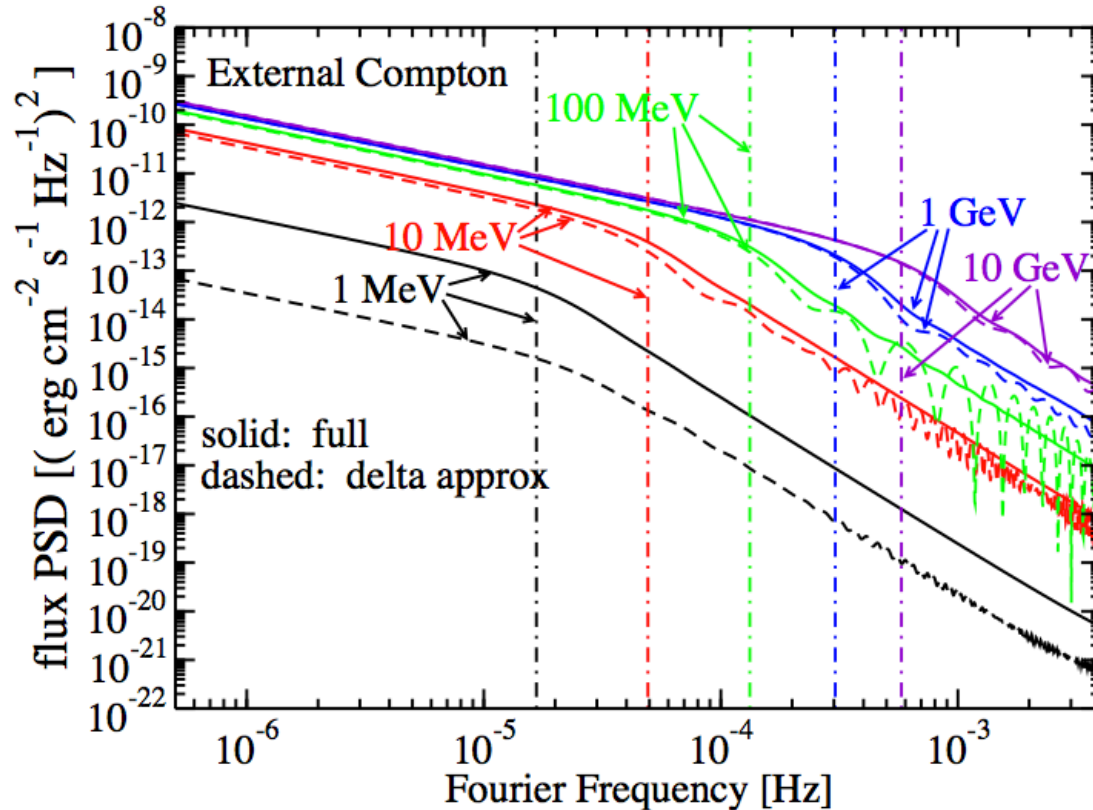


Fig. 2.— The EC PSD for the  $\delta$ -function approximation (Moderski et al. 2005, dashed curves) and full calculation (solid curves). Parameters are the same as in Figure 1. The observed photon energy is shown. Dashed-dotted lines indicate  $f = (1.5t_{\text{cool}})^{-1}$  for each curve.

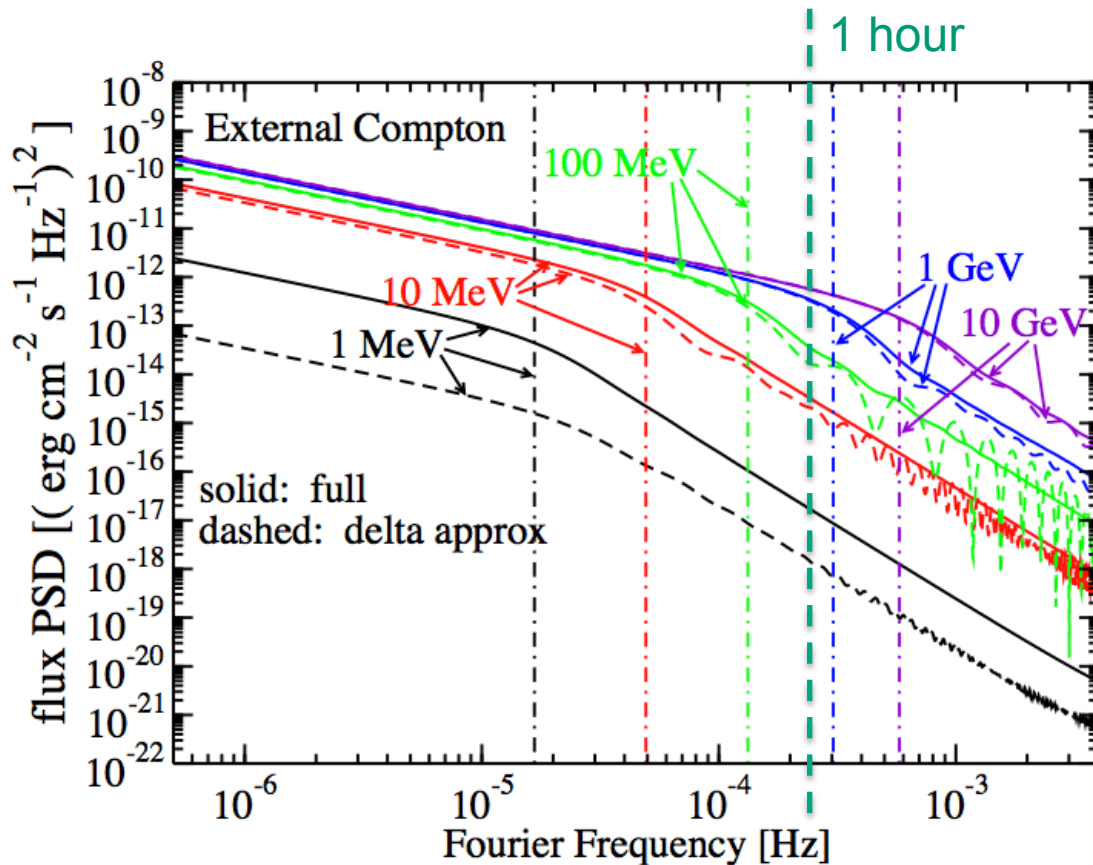
The  $\delta$ -approximation, valid in the Klein-Nishina regime, is from Moderski et al. (2005), MNRAS, 363, 954

Breaks in PSDs can give the observer frame cooling timescale, defined as:

$$t_{\text{cool}}(\epsilon) = \frac{1+z}{\delta_D} \int_{\gamma}^{\infty} \frac{d\gamma'}{|\dot{\gamma}'|}$$

So in principle, we can get the cooling timescale from the PSDs.

# Full Compton cross-section



Breaks in PSDs can give the observer frame cooling timescale, defined as:

$$t_{cool}(\epsilon) = \frac{1+z}{\delta_D} \int_{\gamma}^{\infty} \frac{d\gamma'}{|\dot{\gamma}'|}$$

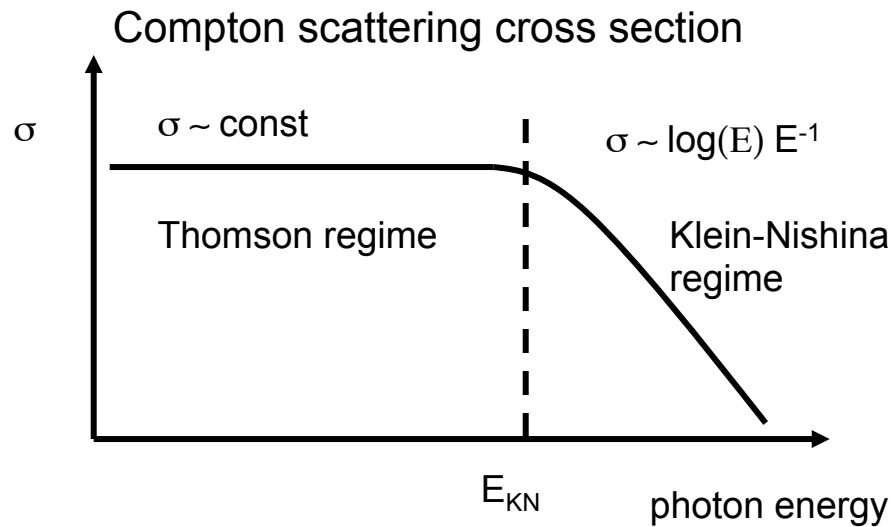
So in principle, we can get the cooling timescale from the PSDs.

Can these breaks be observed?

Fig. 2.— The EC PSD for the  $\delta$ -function approximation (Moderski et al. 2005, dashed curves) and full calculation (solid curves). Parameters are the same as in Figure 1. The observed photon energy is shown. Dashed-dotted lines indicate  $f = (1.5t_{cool})^{-1}$  for each curve.

The  $\delta$ -approximation, valid in the Klein-Nishina regime, is from Moderski et al. (2005), MNRAS, 363, 954

## Finding the location of the emitting region



$$E_{KN} \sim (E_{seed})^{-1}$$

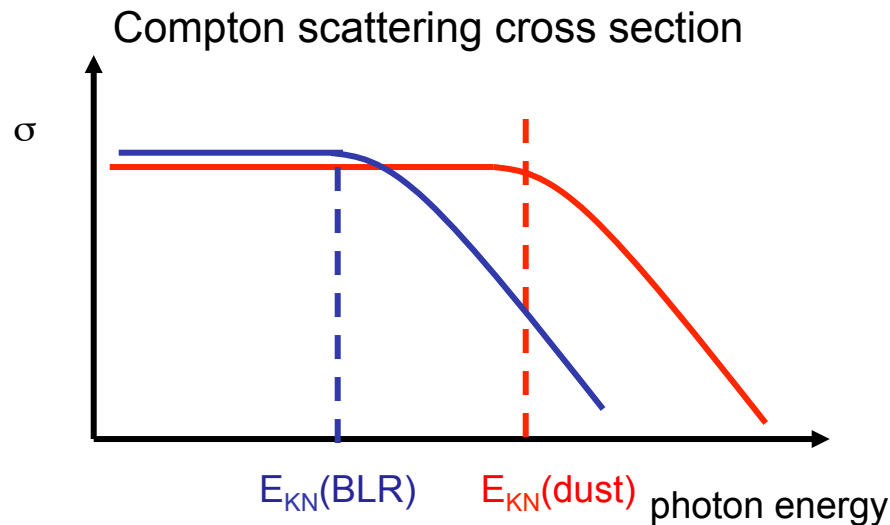
Dust torus:  $10^3$  K black body,  $E_{seed} \sim 0.3$  eV

Ly $\alpha$  broad line:  $E_{seed} \sim 10$  eV

So if you can determine  $E_{KN}$ , one can determine  $E_{seed}$ . But how can you find  $E_{KN}$ ?

**Variability!**

## Finding the location of the emitting region



$$E_{KN} \sim (E_{seed})^{-1}$$

Dust torus:  $10^3$  K black body,  $E_{seed} \sim 0.3$  eV

Ly $\alpha$  broad line:  $E_{seed} \sim 10$  eV

So if you can determine  $E_{KN}$ , one can determine  $E_{seed}$ . But how can you find  $E_{KN}$ ?

### **Variability!**

Scattering dust photons will be more efficient at higher energies, leading to greater cooling and different variability than scattering Ly $\alpha$  photons.

# Compton Dominance



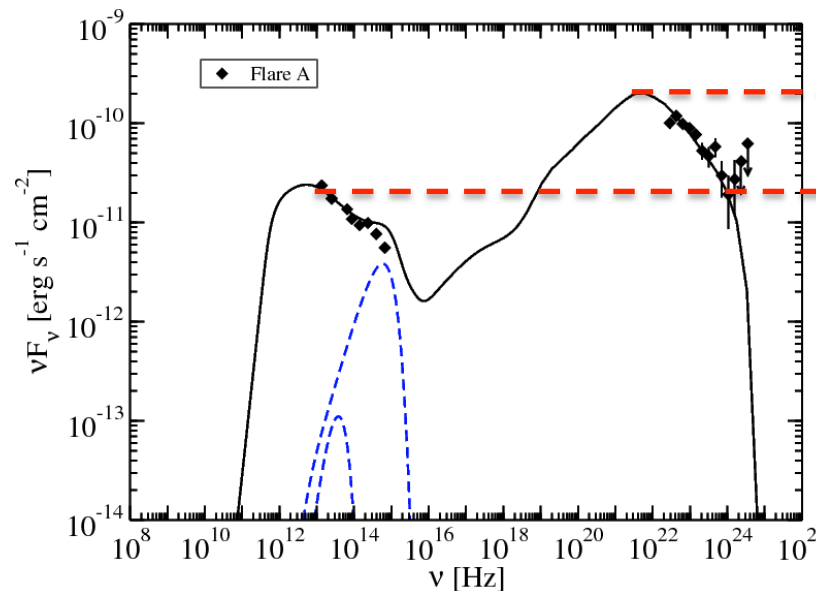
We can develop a function

$$r(\epsilon_a, \epsilon_b, \epsilon_c) = \frac{t_{\text{cool}}(\epsilon_a) - t_{\text{cool}}(\epsilon_c)}{t_{\text{cool}}(\epsilon_a) - t_{\text{cool}}(\epsilon_b)}$$

that depends only on  $\epsilon_0$  and  $A_C$ , where

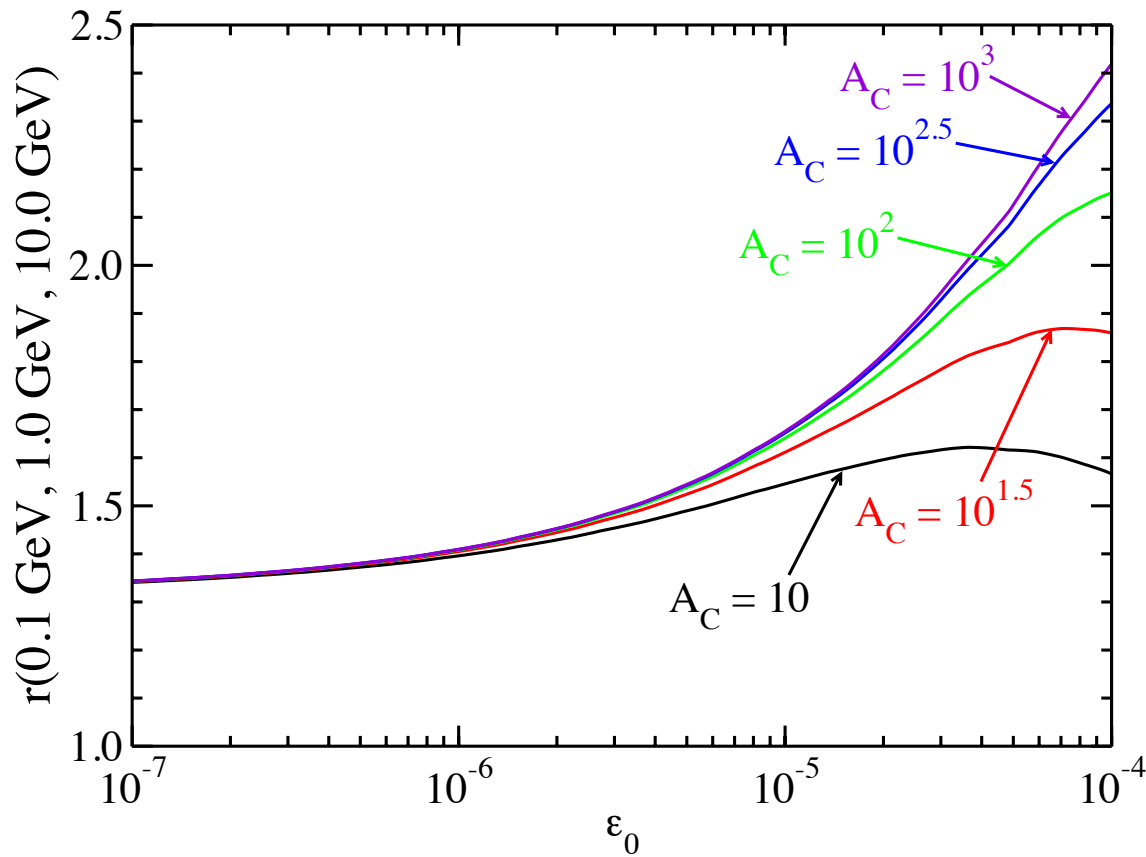
$$A_C = \frac{\Gamma^2 u_0}{u_B}$$

$A_C$  can be determined from broadband SED!



$$A_C = L_C / L_{\text{sy}}$$

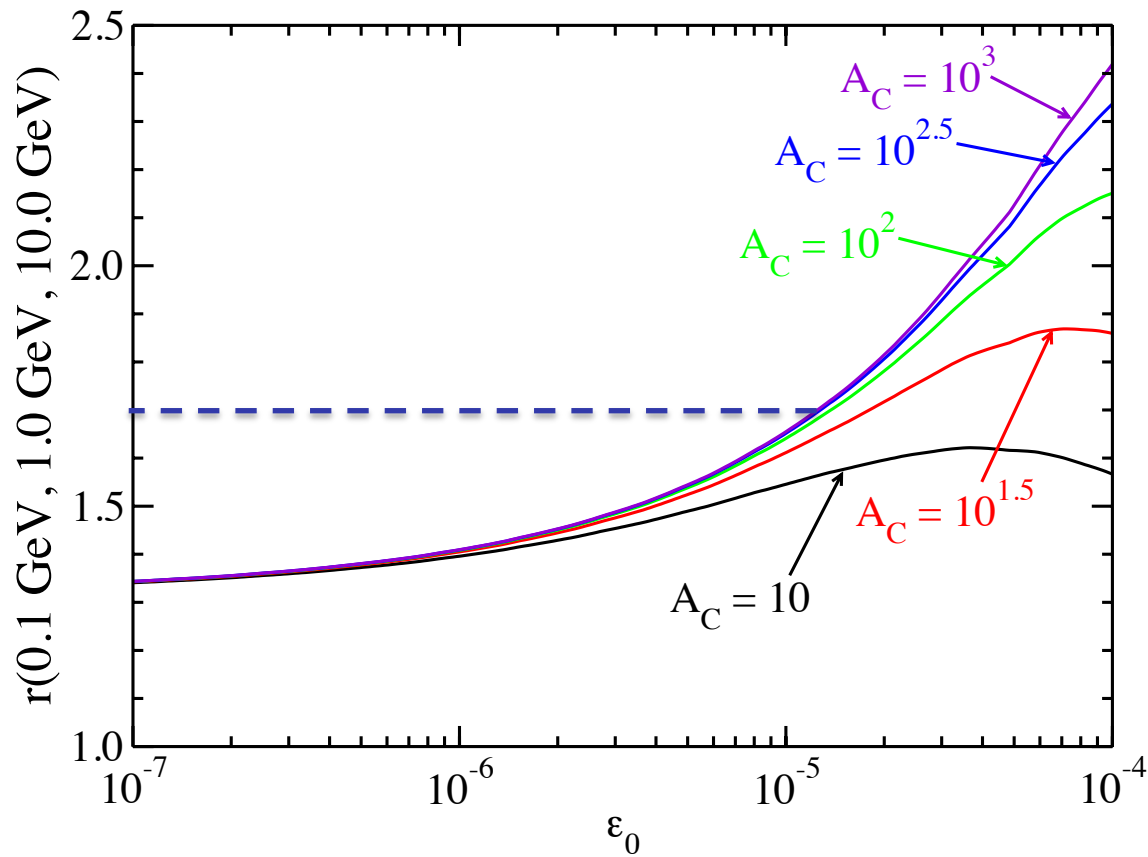
# Full Compton cross-section



$$r(\epsilon_a, \epsilon_b, \epsilon_c) = \frac{t_{\text{cool}}(\epsilon_a) - t_{\text{cool}}(\epsilon_c)}{t_{\text{cool}}(\epsilon_a) - t_{\text{cool}}(\epsilon_b)}$$

$r$  is a function of only observed energies,  $A_C$ , and  $\epsilon_0$ !

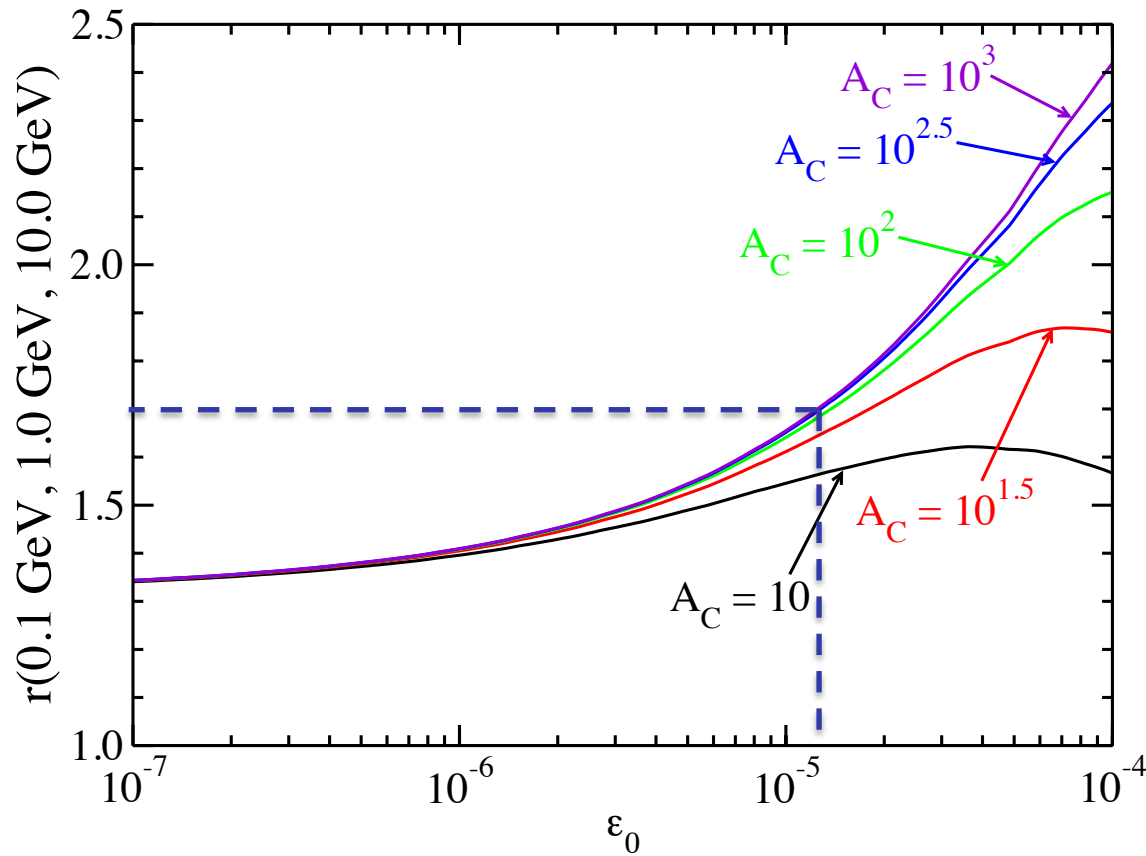
# Full Compton cross-section



$$r(\epsilon_a, \epsilon_b, \epsilon_c) = \frac{t_{\text{cool}}(\epsilon_a) - t_{\text{cool}}(\epsilon_c)}{t_{\text{cool}}(\epsilon_a) - t_{\text{cool}}(\epsilon_b)}$$

$r$  is a function of only  
observed energies,  $A_C$ ,  
and  $\epsilon_0$ !

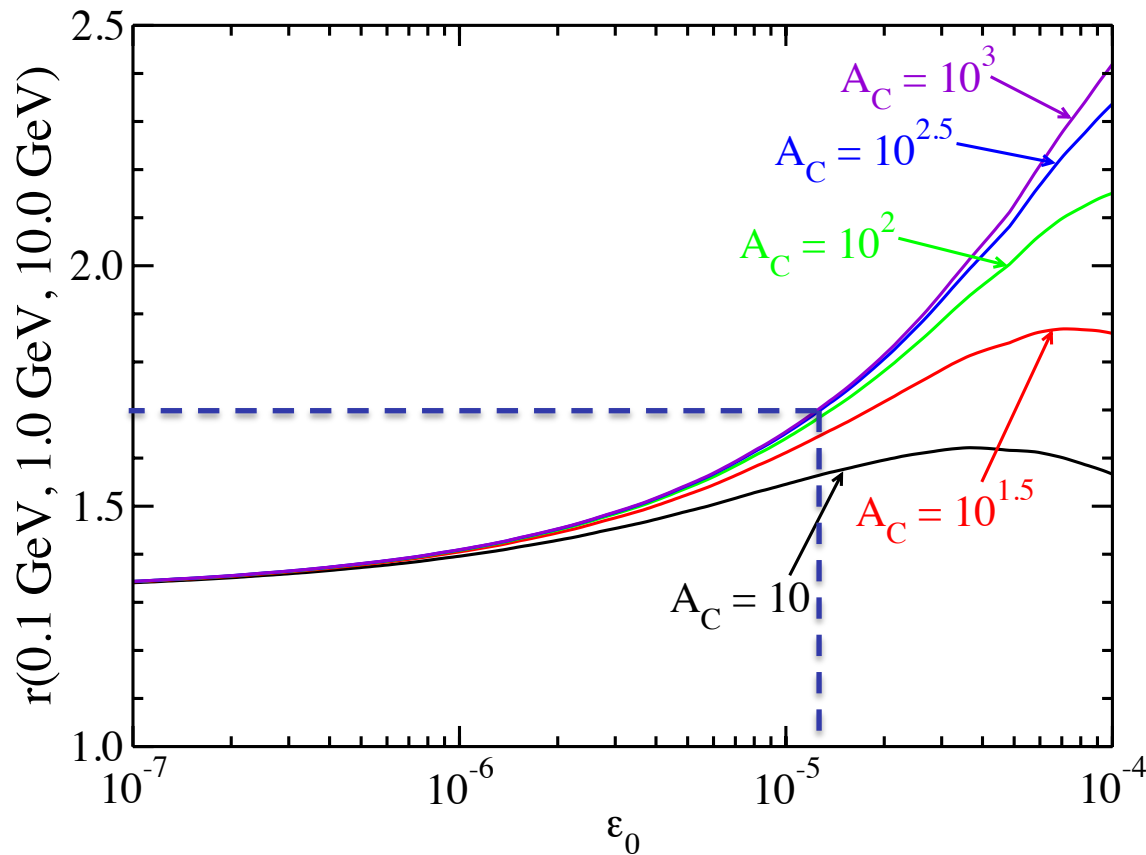
# Full Compton cross-section



$$r(\epsilon_a, \epsilon_b, \epsilon_c) = \frac{t_{\text{cool}}(\epsilon_a) - t_{\text{cool}}(\epsilon_c)}{t_{\text{cool}}(\epsilon_a) - t_{\text{cool}}(\epsilon_b)}$$

$r$  is a function of only  
observed energies,  $A_C$ ,  
and  $\epsilon_0$ !

# Full Compton cross-section



$$r(\epsilon_a, \epsilon_b, \epsilon_c) = \frac{t_{\text{cool}}(\epsilon_a) - t_{\text{cool}}(\epsilon_c)}{t_{\text{cool}}(\epsilon_a) - t_{\text{cool}}(\epsilon_b)}$$

$r$  is a function of only observed energies,  $A_C$ , and  $\epsilon_0$ !

Is it practical to measure the breaks in 3 PSDs of a blazar, each with a different energy bin?

## Time Lags

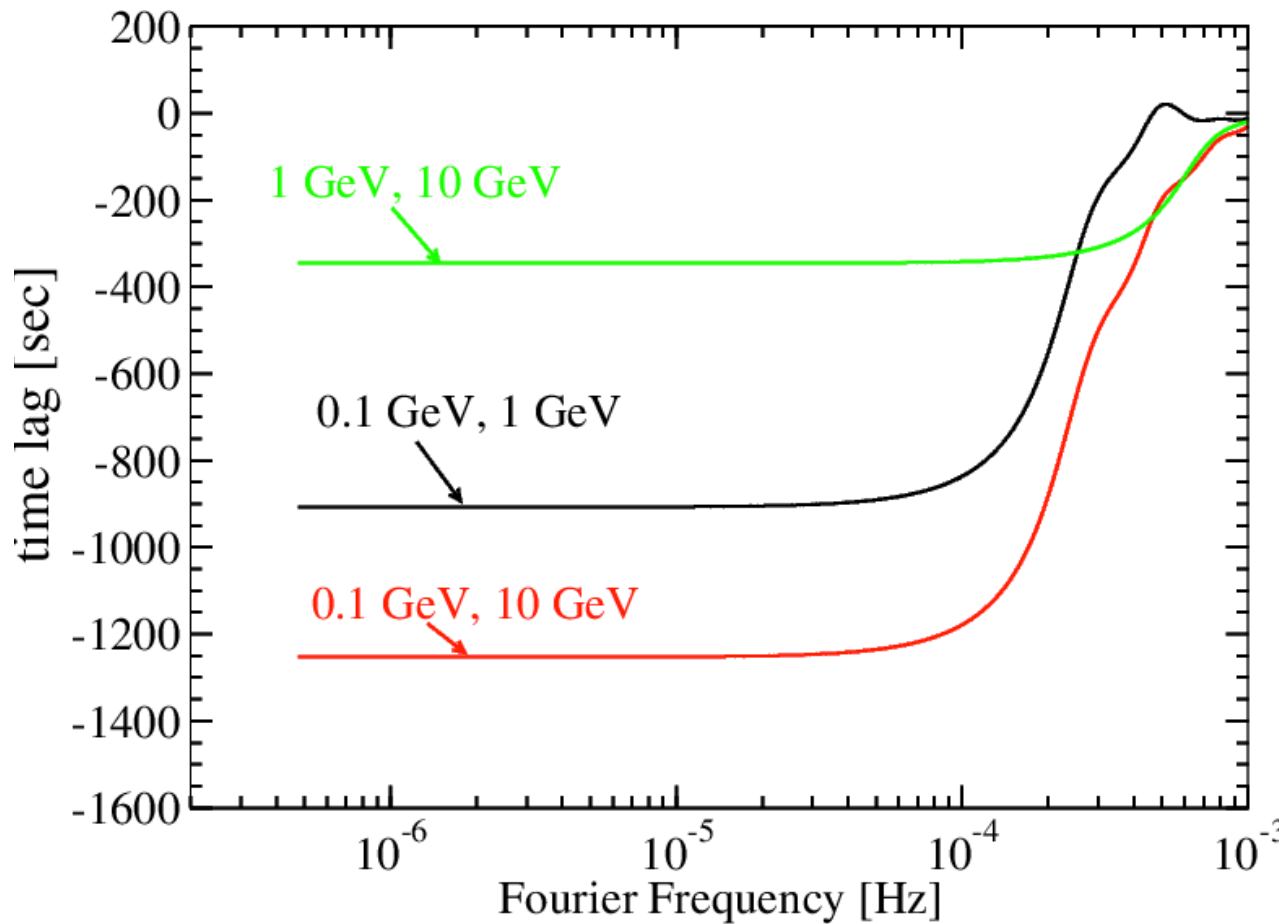


Can also use this model to calculate Fourier frequency-dependent time lags between two channels.

$$\tilde{F}(\epsilon_a, f) \tilde{F}^*(\epsilon_b, f) = Y_R(\epsilon_a, \epsilon_b, f) + i Y_I(\epsilon_a, \epsilon_b, f)$$

$$\Delta T(\epsilon_a, \epsilon_b, f) = \frac{1}{2\pi f} \arctan \left[ \frac{Y_I(\epsilon_a, \epsilon_b, f)}{Y_R(\epsilon_a, \epsilon_b, f)} \right]$$

# Time Lags



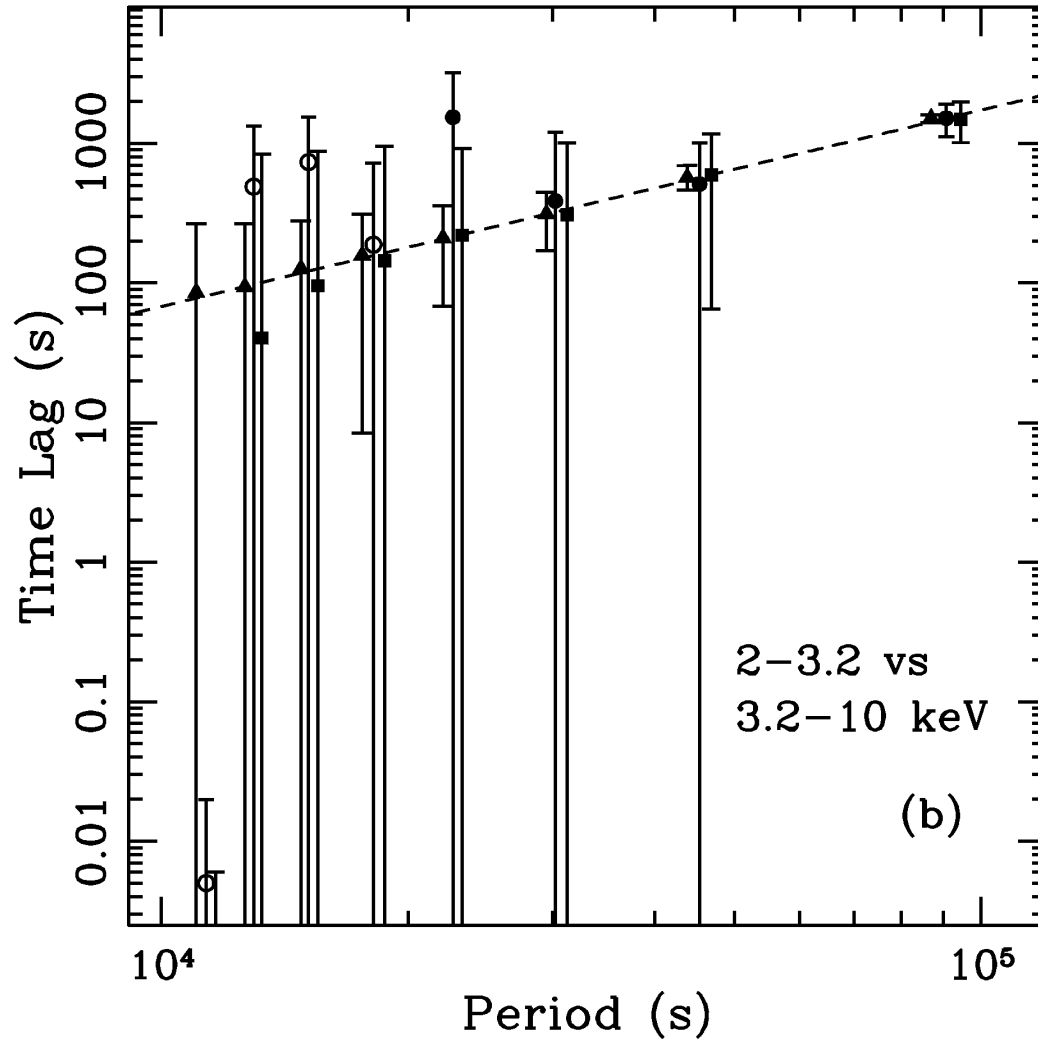
If  $f \ll t_{\text{cool}}/(2\pi)$ , time delay is independent of frequency.

Lags are always soft in this model (soft channel lags behind hard).

A result of longer cooling time for lower energy electrons.

But what is observed?

# Time Lags



Hard lags are observed for Mrk 421 with BeppoSAX!



Second order acceleration, represented by Fokker-Planck equation:

$$\frac{\partial f}{\partial t} = -\frac{1}{p^2} \frac{\partial}{\partial p} \left( p^2 \left[ -D \frac{\partial f}{\partial p} + \langle \dot{p} \rangle_{\text{gain}} f + \langle \dot{p} \rangle_{\text{loss}} f \right] \right) - \frac{f}{t_1} - \frac{f}{t_2(p)} + \frac{N_0 \delta(p - p_0) \delta(t - t_0)}{p_0^2}$$

$$N_e(\gamma; t) \rightarrow p^2 f(p; t)$$

$$\gamma \rightarrow p$$

Hard sphere scattering:

$$D = D_0 p^2$$

$$\langle \dot{p} \rangle_{\text{gain}} = Ap$$

Synchro-Compton losses  
(Thomson regime):

$$\langle \dot{p} \rangle_{\text{loss}} = -\frac{B_0}{mc} p^2$$



Fourier transform:

$$-i\tilde{\omega}F = \frac{1}{x^2} \frac{d}{dx} \left[ x^4 \frac{dF}{dx} - ax^2F - bx^4F \right] - \frac{F}{\tau_1} - \frac{xF}{\tau_2} + \frac{N_0\delta(x - x_0)e^{i\tilde{\omega}y_0}}{(mc)^3 x_0^2}$$

Analytic solution:

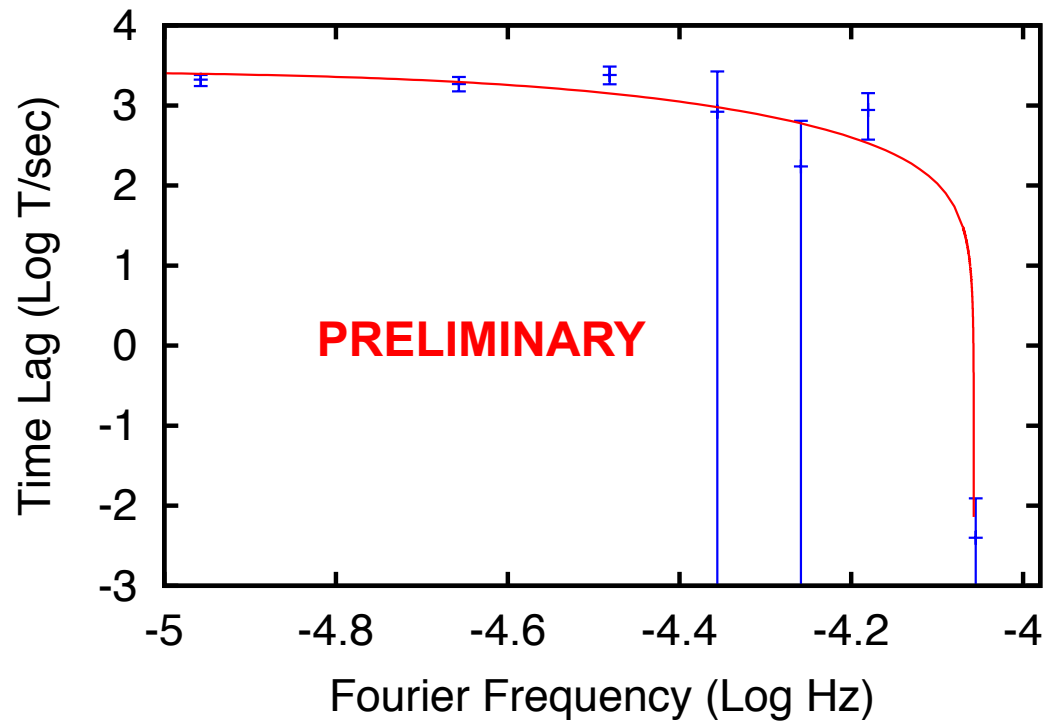
$$F(x) = \frac{N_0}{b(mc)^3} \frac{\Gamma\left(\frac{1}{2} + \mu - \kappa\right)}{\Gamma(1 + 2\mu)} \exp\left[i\tilde{\omega}y_0 + \frac{b}{2}(x_0 - x)\right] x_0^{-2-\frac{a}{2}} x^{-2+\frac{a}{2}} \begin{cases} W_{\kappa,\mu}(bx_0)M_{\kappa,\mu}(bx), & x \leq x_0 \\ M_{\kappa,\mu}(bx_0)W_{\kappa,\mu}(bx), & x \geq x_0 \end{cases}$$

Where W and M are Whittaker functions

# Time Lags



It seems possible to use this model to get a reasonable fit to observed X-ray time lags from Mrk 421 (Zhang 2002):



Doppler factor	$\delta$	21
Magnetic field (G)	$B$	$3.8 \times 10^{-2}$
Comoving blob radius (cm)	$R$	$5.2 \times 10^{16}$

## Summary



- We have created a new theory for the Fourier analysis of blazar variability.
- The simple model assumes variations are only due to changes in the rate of electron injection. Other parameters ( $B$ ,  $u_{\text{ext}}$ ,  $\Gamma$ , etc.) do not change with time.
- LAT  $\gamma$ -ray PSD indices for BL Lacs and FSRQs (Nakagawa & Mori 2013, ApJ, 773, 177) in agreement with theory
- In principle, one can determine  $\varepsilon_0$  from the breaks in several  $\gamma$ -ray PSDs at different energies (Finke & Becker, submitted).
  - Would it be more effective with VHE experiment with large effective area?  
CTA?
- Treatment of particle acceleration will allow reproduction of hard lags (Lewis, Becker & Finke in preparation)



## Extra Slides

## Analytic Solution



$$\gamma^2 \tilde{N}_e(\gamma, f) = Q_0(f/f_0)^{-a/2} \exp \left[ \frac{-1}{v\gamma} \left( \frac{1}{t_{\text{esc}}} - i\omega \right) \right] v^{q-2} \\ \times \left( \frac{1}{t_{\text{esc}}} - i\omega \right)^{1-q} \int_{u_{\text{min}}}^{u_{\text{max}}} du u^{q-2} e^u, \quad (16)$$

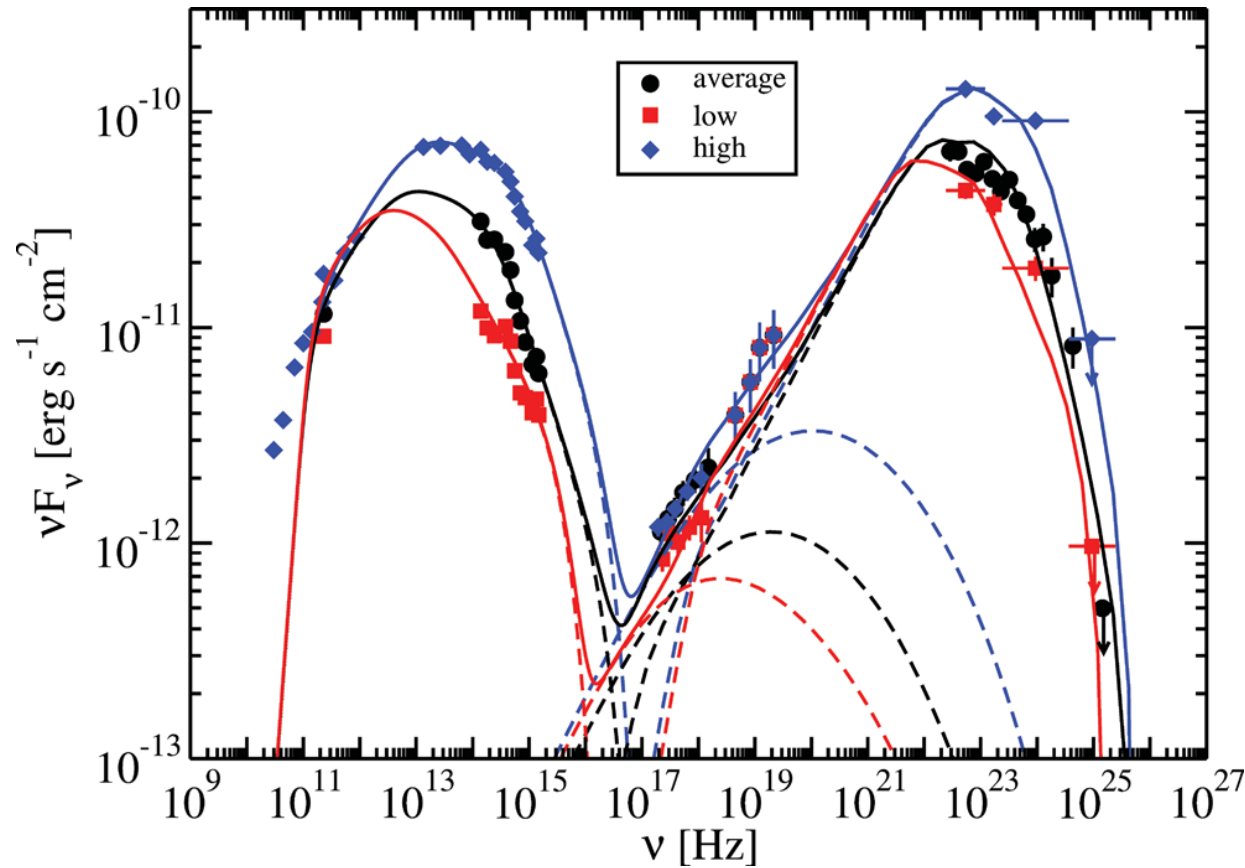
$$u_{\text{min}} = \frac{1}{v\gamma_2} \left( \frac{1}{t_{\text{esc}}} - i\omega \right)$$

$$u_{\text{max}} = \frac{1}{v \max(\gamma, \gamma_1)} \left( \frac{1}{t_{\text{esc}}} - i\omega \right)$$

q=2:

$$\gamma^2 \tilde{N}_e(\gamma, f) = \frac{Q_0(f/f_0)^{-a/2}}{1/t_{\text{esc}} - i\omega} \exp \left[ \frac{-1}{v\gamma} \left( \frac{1}{t_{\text{esc}}} - i\omega \right) \right] \\ \times [e^{u_{\text{max}}} - e^{u_{\text{min}}}],$$

# PKS 0537-441

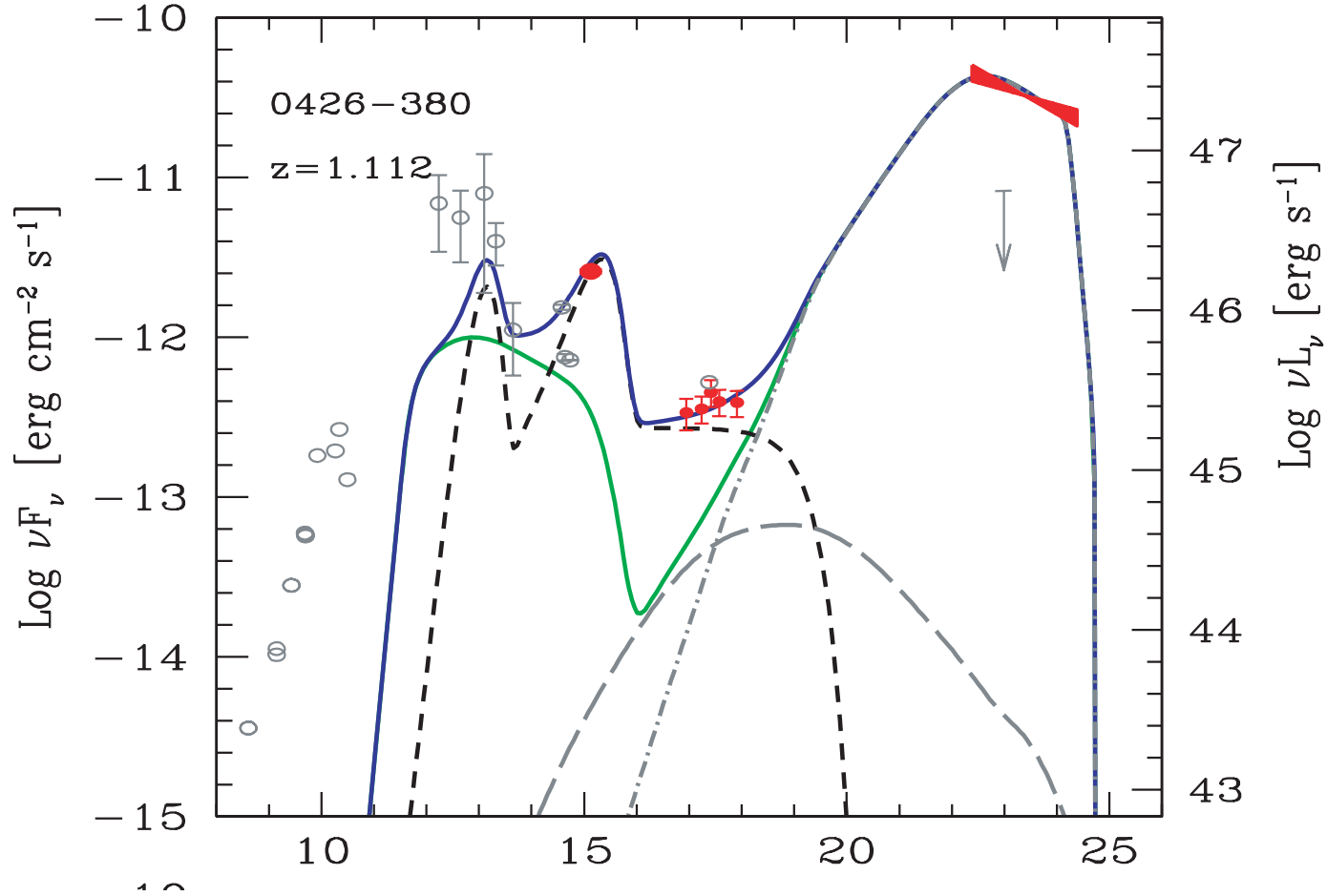


$z=0.896$

D'Ammando et al. (2013), MNRAS, 431, 2481



$z=1.11$



Ghisellini et al. (2009), MNRAS, 399, 2041

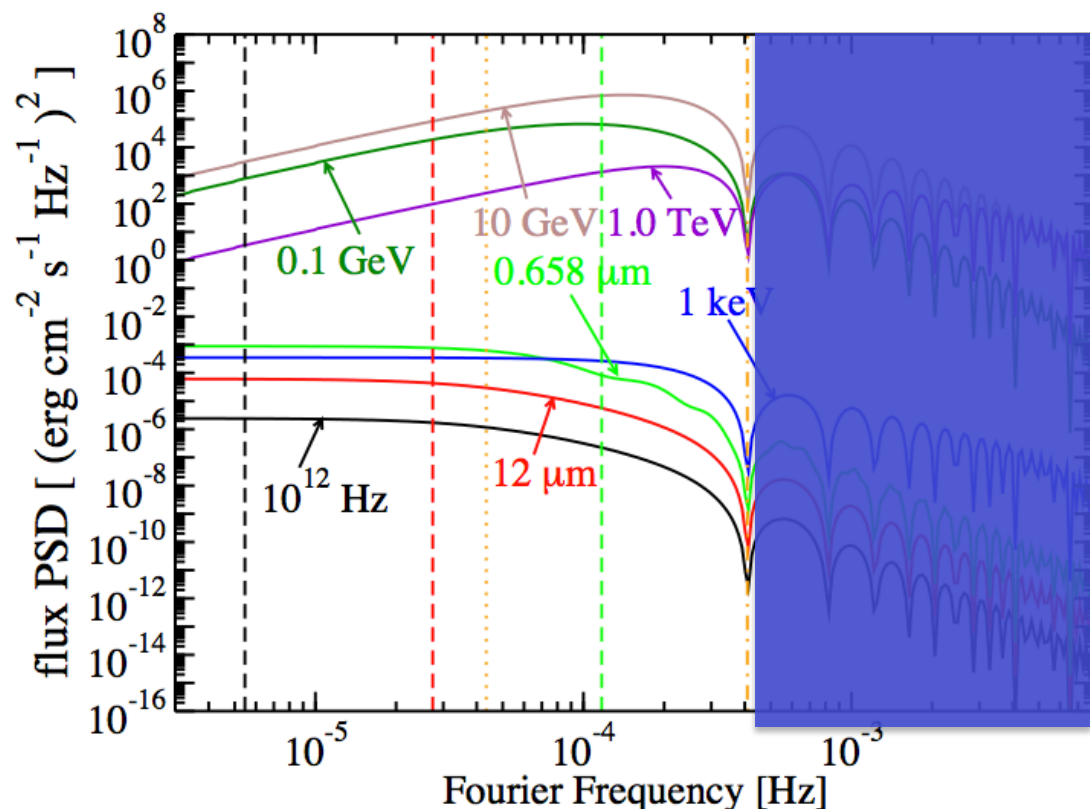


Fig. 6.— The synchrotron and SSC flux PSD computed from Equation (56). Parameters are the same as in Figure 4, except  $u_0 = 0$  and  $z = 0.1$ , giving  $d_L = 1.4 \times 10^{27}$  cm with a cosmology where  $(h, \Omega_m, \Omega_\Lambda) = (0.7, 0.3, 0.7)$ . For the synchrotron curves, the frequency associated with  $t_{\text{cool}}$  for the electrons that produce those photons is shown as the dashed lines. The dotted curve indicates the frequency  $(2\pi t_{\text{esc}})^{-1}$  and the dashed-dotted line indicates the frequency  $t_{\text{lc}}^{-1}$ , all computed in the observer's frame.

Quadratic variability gives different PSD shape. At low frequencies, SSC PSD related to injected electron PSD by:

$$S^{SSC}(\epsilon, f) \propto f^{2-2a}.$$

For synchrotron and EC:

$$S(\epsilon, f) \sim f^{-a}$$

Recall:

$$\tilde{Q}(\gamma, f) = Q_0 (f/f_0)^{-a/2} \gamma^{-q}.$$

# PSD Observer's Summary (so far)



Assuming  $u_B \ll \Gamma^2 u_{\text{ext}}$ , as is likely the case for FSRQs:

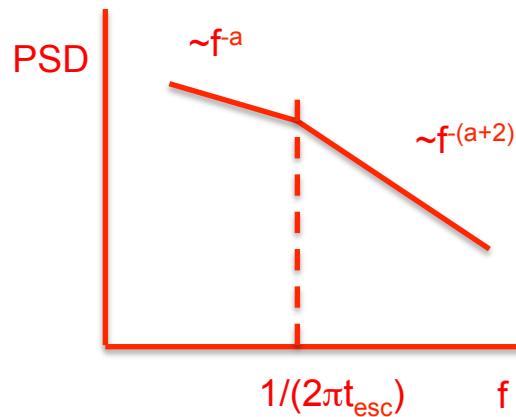
For synch: 
$$\nu_{\text{cr, sy}} = 10^{13} \text{ Hz} \left( \frac{\delta_D}{\Gamma} \right) \left( \frac{\Gamma}{30} \right)^{-3} \left( \frac{u_0}{10^{-3} \text{ erg cm}^{-3}} \right)^{-2} \left( \frac{t_{\text{esc}}}{10^5 \text{ s}} \right)^{-2} \left( \frac{B}{1 \text{ G}} \right) \frac{1}{1+z}$$

For EC: 
$$E_{\text{cr, EC}} = 2 \text{ GeV} \left( \frac{\delta_D}{\Gamma} \right)^2 \left( \frac{\Gamma}{30} \right)^{-2} \left( \frac{u_0}{10^{-3} \text{ erg cm}^{-3}} \right)^{-2} \left( \frac{t_{\text{esc}}}{10^5} \right)^{-2} \left( \frac{\epsilon_0}{2 \times 10^{-5}} \right) \frac{1}{1+z}$$

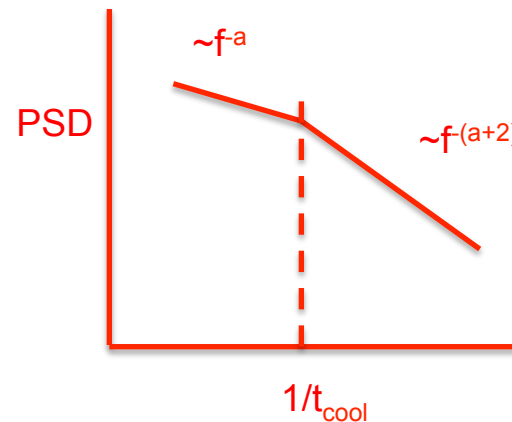
Assuming  $u_B \gg \Gamma^2 u_{\text{ext}}$ , as is likely the case for BL Lacs:

For synch: 
$$\nu_{\text{cr, sy}} = 5 \times 10^{15} \text{ Hz} \left( \frac{\delta_D}{30} \right)^2 \left( \frac{t_{\text{esc}}}{10^5 \text{ s}} \right)^{-2} \left( \frac{B}{1 \text{ G}} \right)^{-3} \frac{1}{1+z}$$

$\nu \ll \nu_{\text{cr}}$   
 $E \ll E_{\text{cr}}$



$\nu \gg \nu_{\text{cr}}$   
 $E \gg E_{\text{cr}}$



## Time Lag Observer's Summary



For synchrotron or EC, at low frequencies, for two channels  $a$  and  $b$ :

$$\left. \begin{array}{l} 1) \text{ If } \nu_{\text{cr}} \ll \nu_a \text{ and } \nu_{\text{cr}} \ll \nu_b \text{ (syn)} \\ \text{or } E_{\text{cr}} \ll E_a \text{ and } E_{\text{cr}} \ll E_b \text{ (EC)} \end{array} \right\} \text{ then } \Delta T(E_a, E_b) = \frac{1}{2}(t_{\text{cool},a} - t_{\text{cool},b})$$

$$\left. \begin{array}{l} 2) \text{ If } \nu_a \ll \nu_{\text{cr}} \ll \nu_b \text{ (syn)} \\ \text{or } E_a \ll E_{\text{cr}} \ll E_b \text{ (EC)} \end{array} \right\} \text{ then } \Delta T(E_a, E_b) = t_{\text{esc}}(1 + \dots)$$

$$\left. \begin{array}{l} 3) \text{ If } \nu_a \ll \nu_{\text{cr}} \text{ and } \nu_b \ll \nu_{\text{cr}} \text{ (syn)} \\ \text{or } E_a \ll E_{\text{cr}} \text{ and } E_b \ll E_{\text{cr}} \text{ (EC)} \end{array} \right\} \text{ then } \Delta T(E_a, E_b) \rightarrow 0$$

See slide 9 for definitions of  $\nu_{\text{cr}}$  and  $E_{\text{cr}}$ .

## Full Compton cross-section



In principle, we can get the cooling timescale from the PSDs. For only synchrotron and EC losses, the ratio of two cooling timescales will be dependent only on the Compton dominance  $A_C$ , and seed photon energy,  $\varepsilon_0$ .

where 
$$A_C = \frac{\Gamma^2 u_0}{u_B}$$

$A_C$  can in principle be determined from a blazar's SED. Can one use the ratio of two cooling timescales to get  $\varepsilon_0$ ? Similar to Dotson et al. (2012), ApJ, 758, 15 .